PROCEEDINGS OF SCIENCE

Delineation of cold and dense two-color QCD with linear sigma model

Daiki Suenaga[a,b,*]

[a] *Kobayashi-Maskawa Institute for the Origin of Particles and the Universe, Nagoya University, Nagoya 464-8602, Japan*

[b] *Research Center for Nuclear Physics (RCNP), Osaka University, Osaka 567-0047, Japan*

E-mail: suenaga.daiki.j1@f.mail.nagoya-u.ac.jp

Two-color ($N_c = 2$) QCD world is one of the useful testing grounds to delineate cold and dense QCD matter, since lattice QCD simulations are straightforwardly applicable thanks to the disappearance of the sign problem. Motivated by recent lattice results, I am being investigating properties of dense two-color QCD theoretically by constructing a new chiral model, the linear sigma model for $N_c = 2$ based on the Pauli-Gürsey $SU(4)$ symmetry. In this write-up, I summarize my recent works on the linear sigma model in dense two-color QCD, such as the hadron mass spectrum and appearance of the sound-velocity peak.

The XVIth Quark Confinement and the Hadron Spectrum Conference (QCHSC24)
19-24 August, 2024
Cairns Convention Centre, Cairns, Queensland, Australia

*Speaker

 ISSN 1824-8039 . Published by SISSA Medialab.

PoS(QCHSC24)201

1. Introduction

Two-color quantum chromodynamics (QCD), i.e., QC_2D, offers a useful testing ground to explore cold and dense matter, since first-principles lattice computations are straightforwardly applicable thanks to disappearance of the sign problem, even in the presence of a chemical potential. In recent years, lattice simulations in dense QC_2D with two flavors ($N_f = 2$) have been being performed by several groups independently [1–4]. Among them, lattice results on the hadron mass spectrum reported by a Japanese group indicated that iso-singlet and 0^- hadron which cannot be described by the chiral perturbation theory (ChPT) [6] turns to be the second-lightest mode at larger chemical potential [5]. In other words, in such a dense regime the ChPT is no longer a reasonable low-energy effective theory. Motivated by this fact I invented a new chiral model, the linear sigma model (LSM) in dense QC_2D, as an extension of the ChPT (For a review please see Ref. [7]). In this write-up, I summarize recent results on, particularly, the hadron mass spectrum [8] and sound-velocity peak [9] in cold and dense QC_2D from my LSM approach.

This article is organized as follows. In Sec. 2 my LSM is introduced, and in Sec. 3 I exhibit numerical results on the hadron mass spectrum and sound velocity. Then, Sec. 4 is devoted to conclusions.

2. Model

In QC_2D, diquarks made of two quarks (qq) become hadrons (baryons) like mesons made of a quark and an antiquark ($\bar{q}q$). Moreover, due to the pseudoreality of $SU(2)$ gauge group, $\mathbf{2} \simeq \bar{\mathbf{2}}$, gluons cannot distinguish quarks and antiquarks. As a result, diquarks and mesons can share common properties. In terms of the chiral representation, such characteristics are reflected as an enlargement of $SU(2)_L \times SU(2)_R$ chiral symmetry to the so-called Pauli-Gürsey $SU(4)$ symmetry [6].

In Ref. [8] I developed a LSM describing mesons and diquarks as the low-energy hadronic excitations of QC_2D collectively, based on the Pauli-Gürsey $SU(4)$ symmetry. The model is of the form

$$\begin{aligned}\mathcal{L}_{\rm LSM} &= \mathrm{tr}[D_\mu \Sigma^\dagger D^\mu \Sigma] - m_0^2 \mathrm{tr}[\Sigma^\dagger \Sigma] - \lambda_1 \left(\mathrm{tr}[\Sigma^\dagger \Sigma]\right)^2 - \lambda_2 \mathrm{tr}[(\Sigma^\dagger \Sigma)^2] \\ &\quad + \bar{c}\,\mathrm{tr}[\zeta^\dagger \Sigma + \Sigma^\dagger \zeta] + \mathcal{L}_{\rm anom.} \,. \end{aligned} \tag{1}$$

In this Lagrangian, Σ is a 4×4 matrix denoting hadron fields of QC_2D:

$$\Sigma = (\mathcal{S}^a - i\mathcal{P}^a) X^a E \,, \tag{2}$$

in which hadrons are embedded as $\eta = \mathcal{P}^0$, $\pi^\pm = (\mathcal{P}^1 \mp i\mathcal{P}^2)/\sqrt{2}$, $\pi^0 = \mathcal{P}^3$, $B = (\mathcal{P}^5 - i\mathcal{P}^4)/\sqrt{2}$, $\bar{B} = (\mathcal{P}^5 + i\mathcal{P}^4)/\sqrt{2}$, $\sigma = \mathcal{S}^0$, $a_0^\pm = (\mathcal{S}^1 \mp i\mathcal{S}^2)/\sqrt{2}$, $a_0^0 = \mathcal{S}^3$, $B' = (\mathcal{S}^5 - i\mathcal{S}^4)/\sqrt{2}$ and $\bar{B}' = (\mathcal{S}^5 + i\mathcal{S}^4)/\sqrt{2}$. Quantum numbers of each hadron are summarized in Table 1. In Eq. (2), E is the 4×4 symplectic matrix while X^a ($a = 0$ - 5) are generators of a subgroup of $U(4)$:

$$E = \begin{pmatrix} 0 & \mathbf{1} \\ -\mathbf{1} & 0 \end{pmatrix}, \quad X^{a=0-3} = \frac{1}{2\sqrt{2}} \begin{pmatrix} \tau_f^a & 0 \\ 0 & (\tau_f^a)^T \end{pmatrix}, \quad X^{a=4,5} = \frac{1}{2\sqrt{2}} \begin{pmatrix} 0 & D_f^a \\ (D_f^a)^\dagger & 0 \end{pmatrix}, \tag{3}$$

where $D^4 = \tau_f^2$ and $D^5 = i\tau_f^2$, with τ_f^a (a = 1 - 3) being the Pauli matrices acting on the flavor space, and $\tau_f^0 = \mathbf{1}$. The matrix form (2) is motivated by a quark bilinear $\Sigma_{ij} \sim \Psi_j^T \sigma^2 \tau_c^2 \Psi_i$ [σ^a and τ_c^a (a = 1 - 3) are the Pauli matrices inhabit the spinor and color spaces, respectively], where Ψ is a four-component spinor $\Psi = (\psi_R, \tilde{\psi}_L)^T$ with $\tilde{\psi}_L = \tau_c^2 \sigma^2 \psi^*$ for $N_f = 2$. Hence, Σ transforms under the $SU(4)$ Pauli-Gürsey transformation as $\Sigma \to g\Sigma g^T$ with $g \in SU(4)$.

In Eq. (1), the covariant derivative is defined by $D_\mu \Sigma = \partial_\mu \Sigma - i\zeta_\mu \Sigma - i\Sigma \zeta_\mu^T$. This ζ_μ and ζ in Eq. (1) are spin-1 and spin-0 spurion fields, respectively, introduced so as to take into account external fields systematically [7]. Thus, $\zeta_\mu \to g\zeta_\mu g^\dagger - i\partial_\mu g g^\dagger$ and $\zeta \to g\zeta g^T$ under $[SU(4)]_{\rm local}$ transformation, for which the whole Lagrangian is invariant under $[SU(4)]_{\rm local}$. In the end, those spurious are replaced by

$$\zeta_\mu \to \delta_{\mu 0} \mu_q J \,, \quad \zeta \to m_q E \,, \tag{4}$$

with $J = \mathrm{diag}(1, 1, -1, -1)$ where μ_q and m_q are a quark-number chemical potential and a current quark mass, respectively. The last term in Eq. (1) is responsible for the $U(1)$ axial anomaly, which generally takes the form of ($\tilde{\Sigma}_{ij} \equiv \frac{1}{2}\epsilon_{ijkl}\Sigma_{kl}$)

$$\mathcal{L}_{\rm anom.} = \frac{a}{2}\mathrm{tr}[\tilde{\Sigma}\Sigma + \tilde{\Sigma}^\dagger \Sigma^\dagger] + \frac{c_1}{4}\left(\mathrm{tr}[\tilde{\Sigma}\Sigma + \tilde{\Sigma}^\dagger \Sigma^\dagger]\right)^2 + \frac{c_2}{2}\mathrm{tr}[\Sigma^\dagger \Sigma]\mathrm{tr}[\tilde{\Sigma}\Sigma + \tilde{\Sigma}^\dagger \Sigma^\dagger] \,. \tag{5}$$

In the following analysis, I will switch off those anomalous contributions as implied by the lattice simulations, $a = c_1 = c_2 = 0$.

As for the ground-state configuration, I leave $\sigma_0 \equiv \langle \mathcal{S}^0 \rangle$ and $\Delta \equiv \langle \mathcal{P}^5 \rangle$ as mean fields, which correspond to the chiral condensate and diquark condensate, respectively. Upon these mean fields, hadron masses are evaluated by taking second derivatives of the Lagrangian (1) with respect to each field, $\mathcal{S}^a$ and $\mathcal{P}^a$.

Table 1: Quantum numbers of the hadrons.

Hadrons	**Spin and parity (J^P)**	**Quark number**	**Isospin**
η	0^-	0	0
π	0^-	0	1
σ	0^+	0	0
a_0	0^+	0	1
B ($\bar{B}$)	0^+	+2 (−2)	0
B' ($\bar{B}'$)	0^-	+2 (−2)	0

3. Numerical results

3.1 Phase transition to the baryon superfluid phase

Phase structures of $\mathrm{QC_2D}$ at finite chemical potential with vanishing temperature is delineated by finding stationary conditions of a potential from the model (1). Within a mean-field

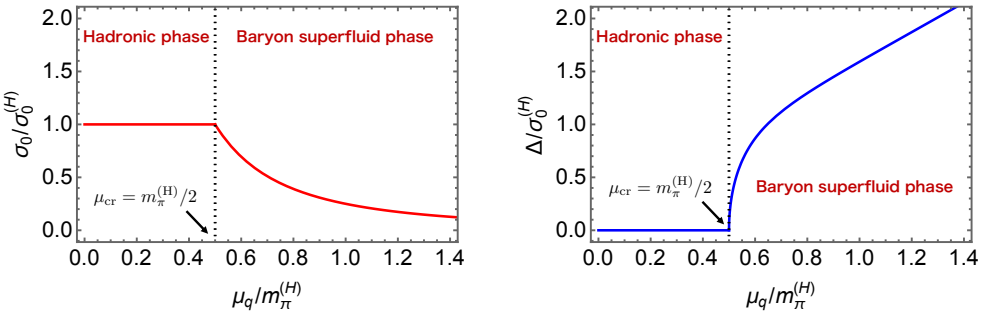

Figure 1: μ_q dependences of the mean fields σ_0 and Δ. The dotted vertical line represents the critical chemical potential $\mu_{\rm cr} = m_\pi^{(\rm H)}/2$ to enter the baryon superfluid phase.

approximation, the potential reads

$$V_{\rm LSM}^{\rm eff} = -2\mu_q^2\Delta^2 + \frac{m_0^2}{2}(\sigma_0^2+\Delta^2) + \frac{\tilde{\lambda}}{4}(\sigma_0^2+\Delta^2)^2 - \sqrt{2}\bar{c}m_q\sigma_0\,, \tag{6}$$

with $\tilde{\lambda} = (4\lambda_1+\lambda_2)/4$. Hence, evaluating $\partial V_{\rm LSM}^{\rm eff}/\partial\sigma_0 = 0$ and $\partial V_{\rm LSM}^{\rm eff}/\partial\Delta = 0$, one can draw μ_q dependences of the mean fields as in Fig. 1. This figure indicates that, when μ_q is adequately small, σ_0 is constant and Δ is always vanishing. Those stable properties are broadly referred to as the *Silver-Blaze properties*. Such a calm phase which is smoothly connected to the vacuum ($T = \mu_q = 0$) is often referred to as the *hadronic phase*. In the hadronic phase, all the meson masses are constant against varying μ_q while (anti)baryon masses linearly decrease (increase) accordingly to their quark numbers, indicating the Silver-Blaze properties. As the chemical potential increases, Δ deviates from zero which leads to the appearance of the Bose-Einstein condensation (BEC) of diquarks. This BEC phase is called the *baryon superfluid phase*. Within the present LSM, the phase transition from the hadronic to superfluid phases is of second-order, and the critical chemical potential is evaluated to be $\mu_{\rm cr} \equiv m_\pi^{(\rm H)}/2$ with $m_\pi^{(\rm H)}$ being a pion mass in the hadronic phase, as indicated in Fig. 1. In the superfluid phase, σ_0 decreases indicating the partial (incomplete) restoration of chiral symmetry.

In obtaining Fig. 1, the following lattice results have been employed as inputs [5]:

$$m_\pi^{(\rm H)} = 738\,{\rm MeV}\,,\quad m_{B'(\bar{B}')}^{(\rm H)} = 1611\,{\rm MeV}\,. \tag{7}$$

Besides, I have adopted $\sigma_0^{(\rm H)} = 250\,{\rm MeV}$ as a typical value for σ_0 in the hadronic phase, and the large N_c limit: $\lambda_1 = 0$.

3.2 Hadron mass spectrum

Depicted in Fig. 2 is a hadron mass spectrum at finite μ_q evaluated by the present LSM, with the inputs explained below Eq. (7). For comparison, I also depict the mass spectrum measured on the lattice in Fig. 3. In the hadronic phase, the Silver-Blaze properties are consistently observed in both the figures. Meanwhile, in the baryon superfluid phase, several noteworthy behaviors are found by the present model for both 0^+ and 0^- hadron masses, so below I will list them by comparing with the lattice results.

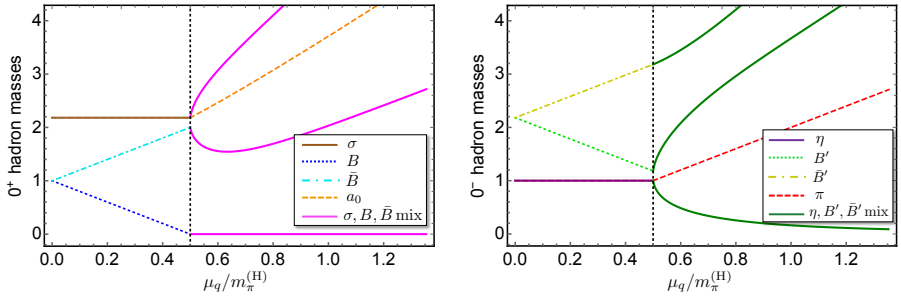

Figure 2: μ_q dependences of masses of the 0^+ hadrons (left) and of the 0^- hadrons (right). The hadron masses are normalized by $m_\pi^{(\mathrm{H})}$. The figures are taken from Ref. [8] where legends are slightly modified.

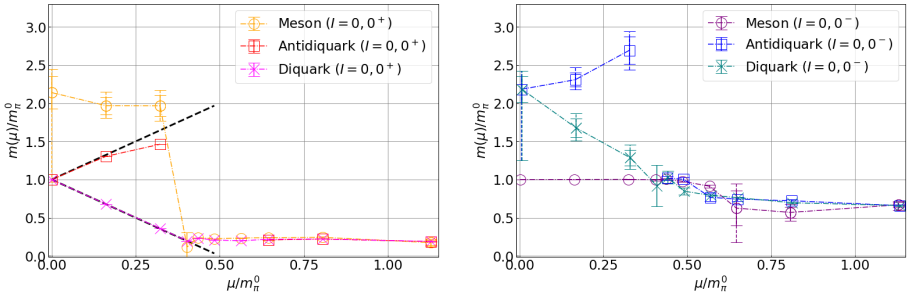

Figure 3: Lattice results of μ_q dependences of masses of the 0^+ hadrons (left) and of the 0^- hadrons (right). The dashed lines in the left panel represent a prediction from chiral models. The figures are taken from Ref. [5].

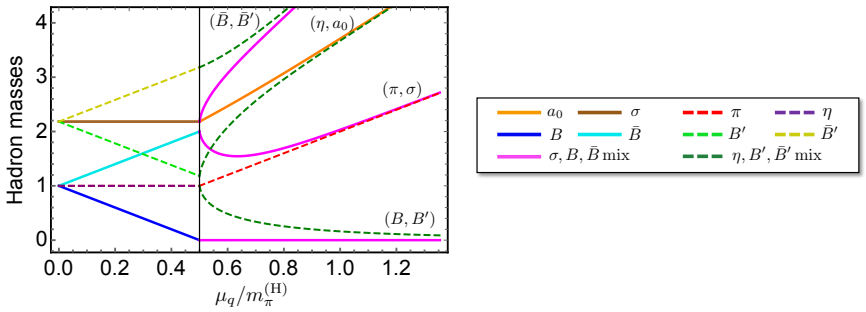

Figure 4: Mass degeneracies of the chiral partners at larger μ_q. The figure is taken from Ref. [8] where legends are slightly modified.

1. The pion mass is analytically evaluated to be $m_\pi = 2\mu_q$ within the model, which would be consistent with the lattice data presented in Ref. [5]. It should be noted that such a simply mass formula seems to be universal among chiral models.

2. Due to the baryon-number (quark-number) violation induced by the appearance of diquark condensates, iso-singlet baryons and mesons carrying common parities mix, resulting in the σ - B - $\bar{B}$ mixed state and η - B' - $\bar{B}'$ mixed state. On the lattice, those mixings are signaled by their mass degeneracies as explicitly shown in Fig. 3.

3. In the left panel of Fig. 2, there appears a massless mode as the lowest state of the σ - B - $\bar{B}$ system. This mode is corresponding to a Nambu-Goldstone (NG) boson associated with the breakdown of $U(1)$ baryon-number symmetry. On the lattice, an approximately massless mode is obtained. Its small mass originates from a fact that the original $U(1)_B$ symmetry is slightly broken due to the presence of a finite diquark source.

4. The lowest state of the η - B' - $\bar{B}'$ system exhibits a nonlinear mass suppression for which this mode turns to be the second-lightest one among all the hadrons. The lattice result, indeed, indicates qualitatively the same μ_q dependence as seen in the right panel of Fig. 3.

In particular, the lattice result on the property 4, i.e., the nonlinear suppression of η - B' - $\bar{B}'$ state, cannot be reproduced by the ChPT where only the pions and 0^+ (anti)diquarks are treated [6]. In this regard, one can conclude that the present LSM but not the ChPT would be a reasonable effective theory in the baryon superfluid phase which is capable of describing low-energy excitations of dense QC_2D correctly.

Finally, I exhibit μ_q dependences of all the hadron masses in Fig. 4. This figure clearly shows mass degeneracies of the chiral partners (parity partners) at large μ_q following the partial restoration of chiral symmetry.

3.3 Sound velocity

In Sec. 3.2 it is found that the present LSM can be regarded as a reasonable effective theory in the superfluid phase of cold and dense QC_2D, from the viewpoint of the mass spectrum of low-energy excitations. Here, as an another probe to judge the usefulness of the LSM, I focus on bulk properties of cold QC_2D matter such as a sound velocity [9].

Within the LSM, the pressure of the system in the baryon superfluid phase takes the following form:

$$p_{\rm LSM} = p_{\rm ChPT} + \delta p \ , \tag{8}$$

where $p_{\rm ChPT}$ is the pressure evaluated within the ChPT ($f_\pi^{(\rm H)} = \sigma_0^{(\rm H)}/\sqrt{2}$)

$$p_{\rm ChPT} = \left(f_\pi^{(\rm H)}\right)^2 \left(m_\pi^{(\rm H)}\right)^2 \left(\bar{\mu} - \frac{1}{\bar{\mu}}\right)^2 \ , \tag{9}$$

and the additional contribution δp reads ($\bar{\mu} \equiv \mu_q/\mu_{\rm cr} = 2\mu_q/m_\pi^{(\rm H)}$)

$$\delta p = \left(f_\pi^{(\rm H)}\right)^2 \left(m_\pi^{(\rm H)}\right)^2 \left[\frac{4}{\delta \bar{m}^2_{\sigma-\pi}} (\bar{\mu}^2 - 1)^2\right] \ , \quad \text{with} \quad \delta \bar{m}^2_{\sigma-\pi} = \frac{\left(m_\sigma^{(\rm H)}\right)^2 - \left(m_\pi^{(\rm H)}\right)^2}{\mu_{\rm cr}^2} \ . \tag{10}$$

In this equation,

$$\left(m_\pi^{(\rm H)}\right)^2 = m_0^2 + \tilde{\lambda}\left(\sigma_0^{(\rm H)}\right)^2 \ , \quad \left(m_\sigma^{(\rm H)}\right)^2 \ = \ m_0^2 + 3\tilde{\lambda}\left(\sigma_0^{(\rm H)}\right)^2 \ , \tag{11}$$

are the masses of pion and σ meson in the hadronic phase. When taking $m_\sigma^{(\rm H)} \to \infty$, the chiral-partner contributions are switched off for which the pressure $p_{\rm LSM}$ is reduced to the ChPT result

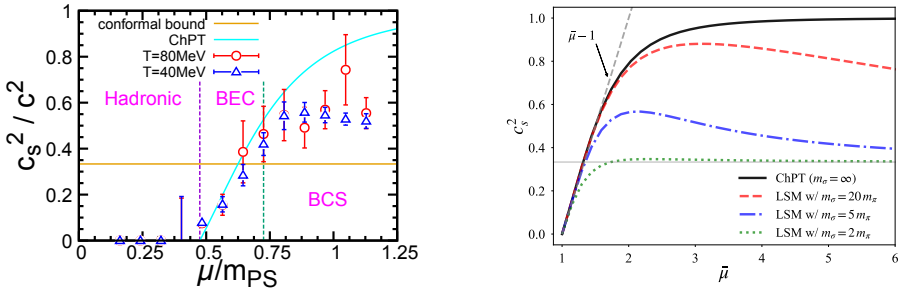

Figure 5: Squared sound velocity measured on the lattice (left) and evaluated within the present LSM in the superfluid phase (right). The left and right figures are taken from Ref. [4] and Ref. [9], respectively.

$p_{\rm ChPT}$. We note that when defining $p_{\rm LSM}$ and $p_{\rm ChPT}$, I have subtracted contributions appropriately such that those pressures vanish in the hadronic phase (i.e., in the vacuum).

From the formula (8) the sound velocity is derived to be

$$\left(c_s^{\rm LSM}\right)^2 = \frac{1}{\mu_q}\frac{\left(\partial p_{\rm LSM}/\partial\mu_q\right)}{\left(\partial^2 p_{\rm LSM}/\partial\mu_q^2\right)} = \frac{\left(1-1/\bar{\mu}^4\right)+8\left(\bar{\mu}^2-1\right)/\delta\bar{m}^2_{\sigma-\pi}}{\left(1+3/\bar{\mu}^4\right)+8\left(3\bar{\mu}^2-1\right)/\delta\bar{m}^2_{\sigma-\pi}}\,. \tag{12}$$

In what follows I will do not employ the inputs explained below Eq. (7). The resultant squared sound velocity in the superfluid phase with several choices of $m_\sigma^{(\rm H)}$ is depicted in the right panel of Fig. 5, while the left panel shows the one measured on the lattice [4]. The lattice result indicates that c_s^2 exceeds the Stefan-Boltzmann limit $(c_s^2)^{\rm SB} = 1/3$ which must be realized at $\mu_q \to \infty$. This excess implies that the sound velocity has peak structures in the superfluid phase. Meanwhile, from the right panel of Fig. 5, the LSM is also capable of yielding such peaks when the mass of σ meson is adequate. We note that c_s^2 is monotonically increases and asymptotically approaches $c_s^2 \to 1$ within the ChPT analysis provided by $m_\sigma^{(\rm H)} \to \infty$ within the LSM description. That is, the ChPT formalism cannot reproduce the peaks of c_s^2. Therefore, again I can conclude from the sound-velocity aspects that the present LSM incorporating chiral partners is regarded as a reasonable effective theory in the baryon superfluid phase [9]. For more quantitative comparison with the lattice data, it is necessary to take into account fluctuation effects and contributions from spin-1 mean fields.

4. Conclusions

In this write-up I have summarized my recent works on the LSM in cold and dense $\mathrm{QC_2D}$ matter, particularly focusing on the spin-0 hadron mass spectrum and sound velocity motivated by the lattice data. Those analyses have indicated that my LSM based on the linear representation of quark bilinears can be regarded as a more reasonable effective theory of dense $\mathrm{QC_2D}$ than the ChPT. In addition to the examinations shown in this article, I also investigated the topological susceptibility [10] to provide theoretical suggestions for inconsistent lattice results [3, 4]. Moreover, in Ref. [4] the model was extended by including spin-1 hadrons in addition to spin-0 ones, and predictions such as possibilities of (axial)vector condensates breaking $O(3)$ rotational symmetry were done based on the Pauli-Gürsey $SU(4)$ symmetry consistently [11]. Therefore, it is expected that our understandings of cold and dense matter would be deepened in the future with further cooperations of the model analysis and lattice simulations.

Acknowledgment

This work was supported by the JSPS KAKENHI Grant No. 23K03377 and No. 23H05439.

References

[1] T. Boz, O. Hajizadeh, A. Maas and J. I. Skullerud, *Finite-density gauge correlation functions in QC2D*, Phys. Rev. D **99**, no.7, 074514 (2019) doi:10.1103/PhysRevD.99.074514 [arXiv:1812.08517 [hep-lat]].

[2] P. V. Buividovich, D. Smith and L. von Smekal, *Electric conductivity in finite-density $SU(2)$ lattice gauge theory with dynamical fermions*, Phys. Rev. D **102**, no.9, 094510 (2020) doi:10.1103/PhysRevD.102.094510 [arXiv:2007.05639 [hep-lat]].

[3] N. Astrakhantsev, V. V. Braguta, E. M. Ilgenfritz, A. Y. Kotov and A. A. Nikolaev, *Lattice study of thermodynamic properties of dense QC_2D*, Phys. Rev. D **102**, no.7, 074507 (2020) doi:10.1103/PhysRevD.102.074507 [arXiv:2007.07640 [hep-lat]].

[4] K. Iida, E. Itou, K. Murakami and D. Suenaga, *Lattice study on finite density QC_2D towards zero temperature*, JHEP **10**, 022 (2024) doi:10.1007/JHEP10(2024)022 [arXiv:2405.20566 [hep-lat]].

[5] K. Murakami, D. Suenaga, K. Iida and E. Itou, *Measurement of hadron masses in 2-color finite density QCD*, PoS **LATTICE2022**, 154 (2023) doi:10.22323/1.430.0154 [arXiv:2211.13472 [hep-lat]].

[6] J. B. Kogut, M. A. Stephanov, D. Toublan, J. J. M. Verbaarschot and A. Zhitnitsky, *QCD - like theories at finite baryon density*, Nucl. Phys. B **582**, 477-513 (2000) doi:10.1016/S0550-3213(00)00242-X [arXiv:hep-ph/0001171 [hep-ph]].

[7] D. Suenaga, *Chiral effective model of cold and dense two-color QCD: The linear sigma model approach*, Symmetry **17**, 124 (2025) doi:10.3390/sym17010124 [arXiv:2502.04496 [hep-ph]].

[8] D. Suenaga, K. Murakami, E. Itou and K. Iida, *Probing the hadron mass spectrum in dense two-color QCD with the linear sigma model*, Phys. Rev. D **107**, no.5, 054001 (2023) doi:10.1103/PhysRevD.107.054001 [arXiv:2211.01789 [hep-ph]].

[9] M. Kawaguchi and D. Suenaga, *Sound velocity peak induced by the chiral partner in dense two-color QCD*, Phys. Rev. D **109**, no.9, 9 (2024) doi:10.1103/PhysRevD.109.096034 [arXiv:2402.00430 [hep-ph]].

[10] M. Kawaguchi and D. Suenaga, *Fate of the topological susceptibility in two-color dense QCD*, JHEP **08**, 189 (2023) doi:10.1007/JHEP08(2023)189 [arXiv:2305.18682 [hep-ph]].

[11] D. Suenaga, K. Murakami, E. Itou and K. Iida, *Mass spectrum of spin-one hadrons in dense two-color QCD: Novel predictions by extended linear sigma model*, Phys. Rev. D **109**, no.7, 074031 (2024) doi:10.1103/PhysRevD.109.074031 [arXiv:2312.17017 [hep-ph]].